Journal of Computational Physics 229 (2010) 2199–2219

Contents lists available at ScienceDirect

Journal of Computational Physics

journal homepage: www.elsevier.com/locate/jcp

Delta function approximations in level set methods by distance function extension

Sara Zahedi *, Anna-Karin Tornberg

School of Computer Science and Communication, Royal Institute of Technology, SE-100 44 Stockholm, Sweden

ARTICLE INFO

Article history:
Received 1 June 2009
Received in revised form 10 November 2009
Accepted 19 November 2009
Available online 27 November 2009

Keywords:
Level set method
Delta function
Consistent approximations
Discretization
Distance function

ABSTRACT

In [A.-K. Tornberg, B. Engquist, Numerical approximations of singular source terms in differential equations, J. Comput. Phys. 200 (2004) 462–488], it was shown for simple examples that the then most common way to regularize delta functions in connection to level set methods produces inconsistent approximations with errors that are not reduced with grid refinement. Since then, several clever approximations have been derived to overcome this problem. However, the great appeal of the old method was its simplicity. In this paper it is shown that the old method – a one-dimensional delta function approximation extended to higher dimensions by a distance function – can be made accurate with a different class of one-dimensional delta function approximations. The prize to pay is a wider support of the resulting delta function approximations.

1. Introduction

The level set method, originally devised by Osher and Sethian [1], is a very popular method for the evolution of interfaces, and it has been implemented for numerous applications. In some of these applications, the question of how to numerically approximate a Dirac delta function arises. For example, in immiscible multiphase problems, Dirac delta functions supported on interfaces separating different fluids are often used in the modeling of the surface tension forces acting on the interfaces. Another example is the problem of evaluating a line integral in two dimensions or a surface integral in three dimensions. This problem can conveniently be reformulated as an integral in 2D or 3D involving a Dirac delta function with support on the line or surface. One approach to approximate such delta functions is to extend a regularized one-dimensional delta function to higher dimensions using a distance function. This has been a common technique in connection to level set methods [2] since the distance function is usually available discretized on a computational grid. However, care is needed since the extension to higher dimensions using a distance function may lead to $\mathcal{O}(1)$ errors [3]. In [3], it was shown that another extension technique that is based on products of regularized one-dimensional delta functions [4] is consistent. This technique is however only applicable when an explicit representation of the curve or the surface is available. In level set methods the curve or the surface is represented implicitly by a level set [2,5].

To overcome the lack of consistency that became apparent with the work presented in [3], a number of consistent delta function approximations that can be used with level set methods have been proposed. Engquist et al. [6] proposed two such approximations. The first one is an approximation of the product rule using the distance function and its gradient. The second one is based on the linear hat function but uses a variable regularization parameter. Smereka [7] derived a discrete delta function obtained as the truncation error in solving the Laplacian of the Green's function, which was proven to be second-order accurate by Beale [8]. Consistent approximations for which the level set function and its gradient are needed have also

* Corresponding author.
E-mail addresses: sara7@kth.se (S. Zahedi), annak@nada.kth.se (A.-K. Tornberg).

0021-9991/$ - see front matter © 2009 Elsevier Inc. All rights reserved.
doi:10.1016/j.jcp.2009.11.030

been introduced by Towers [9,10]. The advantage of these methods is that the supports of the delta function approximations are very small. The discrete delta function proposed by Smereka has its support contained within a single mesh cell.

One way to explain the reason for the inconsistency shown in [3] is the following: The one-dimensional delta function approximation is designed to obey certain moment conditions on a uniform grid. The first moment condition is the mass condition that ensures that the delta function approximation sums to one independent of shifts in the grid. Delta function approximations with compact support where the widths of the approximations are fixed to a number of cell widths was considered in [3]. As the one-dimensional delta function is extended to higher dimensions, using the closest distance to the line or surface, the effective width in each coordinate direction relative to the grid size will depend on the slope of the curve or surface. This will in general no longer be within the design of the one-dimensional delta approximation, causing a violation of the mass condition, and hence an $\mathcal{O}(1)$ error that will not vanish with grid refinement. This is further discussed in Section 3. This effect was recognized by Engquist et al. [6] who introduced a first correction to this, by defining the regularization parameter to depend on the gradient of the distance function.

The problem with extending the delta function to higher dimensions using the closest distance to the line or surface is hence that the one-dimensional delta approximation is dilated, and that the moment conditions are no longer valid. One can however construct delta approximations such that the moment conditions do hold for a wide range of dilations. These functions are however not of compact support. One such function was given in [11]. It has compact support in Fourier space, and decays rapidly enough in real space to lend itself to truncation, but the effective support will be wider than one or two grid points as in the approximations above. In addition, in difference to the delta function approximations discussed above, that are of low regularity, this function is infinitely differentiable.

In the analysis in [12], the error is split into two parts. The first part is the analytical error due to the approximation of the delta function. The second part is the numerical error due to the approximation of the integral containing the delta function approximation. For the first part, it is continuous moment conditions that are important, and for the second part, it is (in addition to the order of the quadrature rule) the regularity of the delta function approximation that limits the accuracy. This gives an upper limit of the error, but in the case when extending by the distance rule, the error is typically quite close to this upper limit. The result from this analysis is that the numerical error is of order $\mathcal{O}((h/\varepsilon)^p)$ where p is determined by the regularity of the delta function approximation. For the compact one-dimensional delta function approximation, the regularity is typically low. With a choice of $\varepsilon = mh$, which has been the common choice, the numerical error is of $\mathcal{O}(1)$, and the method is inconsistent. Depending on the regularity and continuous moment order of the approximation, there is an optimal $\alpha < 1$ in $\varepsilon \sim h^\alpha$ that results in the best convergence. If we replace the narrow delta function approximation with an infinitely differentiable delta function approximation, the result is quite different. The regularity of the delta function approximation will no longer limit the accuracy of the quadrature rule. In fact, these functions can be considered as periodic functions, since they decay to zero. For these functions, the trapezoidal rule on a uniform grid will converge faster than any power of h in the limit as $h \to 0$. This is often referred to as the superconvergence of the trapezoidal rule, and will yield a very small numerical error.

In this paper, we will consider three different functions that all have these properties. We will now provide a comparison between one of the delta function approximations considered in this paper and the narrow linear hat function which in [3] was shown to give $\mathcal{O}(1)$ errors. Consider the computation of the arc-length of a circle of radius 1 centered at the origin by evaluating

$$\int_\Omega \delta_\varepsilon(d(\Gamma,\mathbf{x}))d\Omega,$$

where the computational domain Ω is discretized with a regular mesh with mesh size h. Use the trapezoidal rule for the integration. For the narrow linear hat function

$$\delta^L_{2h}(x) = \begin{cases} \frac{1}{2h}\left(1 - \frac{|x|}{2h}\right), & \text{if } |x| \leqslant 2h, \\ 0, & \text{if } |x| > 2h, \end{cases} \tag{1}$$

there is no analytical error in the computation of the arc-length, see [12]. Still there is no convergence as $h \to 0$:

h	0.1	0.05	0.025	0.0125	0.00625
Relative error	2.2×10^{-3}	8×10^{-4}	8×10^{-4}	5×10^{-4}	4×10^{-4}

Due to the symmetry of the problem and resulting cancellation of errors, these errors are quite small compared to the errors in the examples given in Section 3. We use the same technique with the one-dimensional delta function $\delta_\varepsilon(x) = \delta^{FD}_{2h}(x)$ defined as the derivative of the Fermi–Dirac function

$$\delta^{FD}_{2h}(x) = \partial_x \frac{1}{1 + e^{-x/(2h)}}. \tag{2}$$

This delta function approximation was used in the conservative level set method [13,14]. For this approximation, the error decreases exponentially down to the relative floating point error:

h	0.1	0.05	0.025	0.0125	0.00625
Relative error	4.4×10^{-3}	2×10^{-5}	7×10^{-10}	1×10^{-14}	4×10^{-15}

What we see is the superconvergence of the trapezoidal rule for infinitely differentiable periodic functions.

This paper is organized as follows. In Section 2 we define delta function approximations and state conditions for accuracy in one dimension. In Section 3 we discuss the simple example of computing the length of a line. We show why the compact delta function approximations produce $O(1)$ errors and how large they are. We also show why this does not occur for approximations with compact support in Fourier space. In Section 4 we introduce three different consistent delta function approximations and discuss their properties. In Section 5 we state and prove theorems for the error in both two and three dimensions. We present numerical experiments in Section 6 and summarize our results in Section 7.

2. Regularization

Given a continuous function $\varphi(\xi)$, a delta function approximation can be constructed by

$$\delta_\varepsilon(x) = \frac{1}{\varepsilon}\varphi(x/\varepsilon). \tag{3}$$

Examples of such $\varphi(\xi)$ functions with compact support are: the piecewise linear hat function

$$\varphi^L(\xi) = \begin{cases} (1-|\xi|), & \text{if } |\xi| \leqslant 1, \\ 0, & \text{if } |\xi| > 1, \end{cases} \tag{4}$$

the cosine approximation

$$\varphi^{\cos}(\xi) = \begin{cases} \frac{1}{2}(1+\cos(\pi\xi)), & \text{if } |\xi| \leqslant 1, \\ 0, & \text{if } |\xi| > 1, \end{cases} \tag{5}$$

and the piecewise cubic function

$$\varphi^C(\xi) = \begin{cases} 2-|2\xi|-2|2\xi|^2+|2\xi|^3, & \text{if } 0 \leqslant |\xi| \leqslant 1/2, \\ 2-\frac{11}{3}|2\xi|+2|2\xi|^2-\frac{1}{3}|2\xi|^3, & \text{if } 1/2 < |\xi| \leqslant 1, \\ 0, & \text{if } |\xi| > 1. \end{cases} \tag{6}$$

The functions $\varphi^L(\xi), \varphi^{\cos}(\xi)$, and $\varphi^C(\xi)$ are plotted in Fig. 1.

In the next section we state the conditions which the regularized one-dimensional delta function must satisfy in order to be accurate.

2.1. Discrete regularization in one dimension

Assume a regular grid in one dimension, with grid size h and grid points $x_j = jh, j \in \mathbb{Z}$. We introduce the discrete moment conditions:

Definition 2.1. A function δ_ε satisfies q discrete moment conditions if for all $x^* \in \mathbb{R}$,

$$M_r(\delta_\varepsilon, x^*, h) = h\sum_{j\in\mathbb{Z}} \delta_\varepsilon(x_j - x^*)(x_j - x^*)^r = \begin{cases} 1, & \text{if } r = 0, \\ 0, & \text{if } 1 \leqslant r < q, \end{cases} \tag{7}$$

where $x_j = jh, h > 0, j \in \mathbb{Z}$.

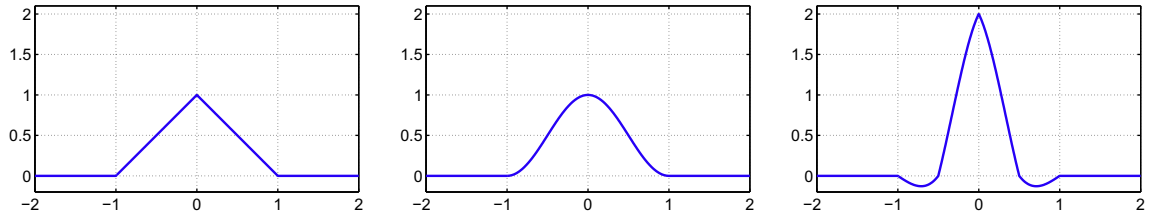

(a) $\varphi^L(\xi)$ (b) $\varphi^{\cos}(\xi)$ (c) $\varphi^C(\xi)$

Fig. 1. Building blocks $\varphi(\xi)$ for delta function approximations. A linear hat function (a), a cosine approximation (b), and a piecewise cubic function (c).

If δ_ε satisfies q moment conditions, we say that it has a moment order q. The first moment condition ensures that the mass of the delta function approximation δ_ε is one, independent of shifts in the grid. It is therefore referred to as the mass condition. The higher moment conditions are important when the delta approximation is multiplied by a non-constant function. The following theorem states that in one dimension the numerical accuracy of a regularized delta function is determined by the number of discrete moment conditions.

Proposition 2.1. *Assume δ_ε satisfies q discrete moment conditions and has compact support in $[-Mh, Mh]$. Assume also that $f(x) \in C^q(\mathbb{R})$, and that all derivatives of f are bounded, then*

$$E = \left| h \sum_j \delta_\varepsilon(x_j - x^*) f(x_j) - f(x^*) \right| \leqslant Ch^q \tag{8}$$

and $E = 0$ if f is constant.

A proof based on Taylor expansion of f around $x^* \in \mathbb{R}$ is found in Refs. [3,15]. The delta function approximations δ_ε in last section have support in $[-\varepsilon, \varepsilon]$. The linear hat function $\delta^L_{2h}(x)$, the cosine approximation $\delta^{\cos}_{2h}(x)$ and the cubic function $\delta^C_{2h}(x)$ all satisfy the mass condition and hence are consistent approximations. The cubic function $\delta^C_{2h}(x)$ is most accurate. It satisfies four discrete moment conditions and is according to Proposition 2.1 a fourth-order accurate approximation.

2.2. Extensions to higher dimensions

A Dirac delta measure concentrated on a curve or surface can be approximated by extending a regularized one-dimensional delta function to higher dimensions. Basically two techniques are used. One is the product formula and the other technique is based on a distance function to the curve or the surface.

Let $\Gamma \subset \mathbb{R}^d$ be a $d-1$ dimensional closed, continuous, and bounded surface and let S be a parametrization of Γ. Define $\delta(\Gamma, g, \mathbf{x})$ as a delta function of variable strength supported on Γ such that

$$\int_{\mathbb{R}^d} \delta(\Gamma, g, \mathbf{x}) f(\mathbf{x}) d\mathbf{x} = \int_\Gamma g(S) f(\mathbf{X}(S)) dS, \tag{9}$$

where $\mathbf{x} = (x^{(1)}, \ldots x^{(d)}) \in \mathbf{R}^d$ and $\mathbf{X}(S) = (X^{(1)}(S), \ldots, X^{(d)}(S)) \in \Gamma$.

The product formula yields

$$\delta_{\boldsymbol{\varepsilon}}(\Gamma, g, \mathbf{x}) = \int_\Gamma \prod_{k=1}^{d} \delta_{\varepsilon_k}(x^{(k)} - X^{(k)}(S)) g(S) dS, \tag{10}$$

where δ_{ε_k} is a one-dimensional regularized delta function.

Assume that the space $\mathbb{R}^d$ is covered by a regular grid

$$\{\mathbf{x_j}\}_{\mathbf{j} \in \mathbb{Z}^d}, \quad \mathbf{x_j} = \left(x^{(1)}_{j_1}, \ldots, x^{(d)}_{j_d}\right), \quad x^{(k)}_{j_k} = x^{(k)}_0 + j_k h_k, \quad j_k \in \mathbb{Z}, \quad k = 1, \ldots, d. \tag{11}$$

The following theorem was proved by Tornberg and Engquist in Ref. [3].

Theorem 2.1. *Suppose that δ_ε is a one-dimensional delta function approximation with compact support in $[-\varepsilon, \varepsilon]$, that satisfies q discrete moment conditions (see Definition 2.1); $g \in C^r(\mathbb{R}^d)$ and $f \in C^r(\mathbb{R}^d), r \geqslant q$. Then for any rectifiable curve Γ and $\delta_{\boldsymbol{\varepsilon}}(\Gamma, g, \mathbf{x})$ as defined in* Eq. (10) *with $\boldsymbol{\varepsilon} = (mh_1, mh_2, \ldots, mh_d)$, it holds that*

$$E = \left| \left(\prod_{k=1}^{d} h_k \right) \sum_{j \in \mathbb{Z}^d} \delta_\varepsilon(\Gamma, g, \mathbf{x}_j) f(\mathbf{x}_j) - \int_\Gamma g(S) f(\mathbf{X}(S)) dS \right| \leqslant Ch^q \tag{12}$$

with $h = \max_{1 \leqslant k \leqslant d} h_k$ and $E = 0$ for constant f.

This means that the results from one dimension carry over to higher dimensions, and that it is still the discrete moment order of the one-dimensional delta function approximation that determines the order of accuracy.

The product formula is easy to use when Γ is explicitly defined. However, in level set methods, Γ is defined implicitly by a level set function $\phi(\mathbf{x}) : \mathbb{R}^d \to \mathbb{R}$,

$$\Gamma = \{\mathbf{x} : \phi(\mathbf{x}) = 0\}. \tag{13}$$

It is therefore preferable to use this function to extend the regularized one-dimensional delta function δ_ε to higher dimensions. In the case when $\phi(\mathbf{x}) = d(\Gamma, \mathbf{x})$, a signed distance function to Γ, where the distance is the Euclidean distance from $\mathbf{x}$ to Γ, the delta function approximation is defined as

$$\delta_\varepsilon(\Gamma, g, \mathbf{x}) = \tilde{g}(\mathbf{x}) \delta_\varepsilon(d(\Gamma, \mathbf{x})), \tag{14}$$

where $\tilde{g}$ is a smooth extension of g to $\mathbb{R}^d$, such that $\tilde{g}(X(S)) = g(S)$. Using the level set function the integral in Eq. (9) can be written as

$$\int_{\mathbb{R}^d} f(\mathbf{x})\delta(\Gamma, g, \mathbf{x})d\mathbf{x} = \int_{\mathbb{R}^d} f(\mathbf{x})\tilde{g}(\mathbf{x})\delta(\phi(\mathbf{x}))|\nabla\phi(\mathbf{x})|d\mathbf{x}. \tag{15}$$

Note that the extra scaling of $|\nabla\phi|$ is needed when ϕ is not a distance function. In this paper we focus on the extension to higher dimensions that employs the distance function.

3. Computing the length of a straight line

In this section we study the error made in the computation of the length of a straight line. In the computations a regularized one-dimensional delta function δ_ε is extended to higher dimensions using a distance function, according to Eq. (14) with $\tilde{g} = 1$.

Consider the problem of calculating the length of a curve Γ:

$$|\Gamma| = \overline{S} = \int_{\mathbb{R}^2} \delta(\Gamma, \mathbf{x})d\mathbf{x}. \tag{16}$$

In the computation of $|\overline{S}|$, a delta function approximation δ_ε on a regular grid is used:

$$\overline{S}_h = h^2 \sum_{j\in\mathbb{Z}^2} \delta_\varepsilon(d(\Gamma, \mathbf{x_j})), \quad \mathbf{x_j} = (x_{j_1}, y_{j_2}), \quad x_{j_1} = j_1 h, \quad y_{j_2} = j_2 h, \quad j_l \in \mathbb{Z}, \quad l = 1, 2. \tag{17}$$

In the following we will let the curve $\Gamma \in \mathbb{R}^2$ be a straight line with slope k, but not a vertical line or a horizontal line. In Ref. [3] it was shown that for $\Gamma = \{\mathbf{x}, x^{(2)} = x^{(1)}, 0 \leqslant x^{(1)} < \overline{S}/\sqrt{2}\}$, a line with slope $k = 1$ and δ_ε being equal to the narrow linear hat function δ_h^L the relative error $|\overline{S}_h - \overline{S}|/\overline{S}$ is more than 12% as $h \to 0$. This was shown by dividing the sum $\overline{S}_h$ into contributions of M subsegments of Γ, each of length $\sqrt{2}h$. Here, we consider a different approach. We express the error in terms of the first discrete moment of δ_ε (see Eq. (7) with $r = 0$). We can then show which delta function approximations that will produce $\mathcal{O}(1)$ errors. For simplicity, we consider a line of infinite length so we do not have to worry about contributions from end point terms.

From Eq. (3) we see that we can write $\delta_\varepsilon(x)$ as

$$\delta_\varepsilon(x) = \eta\delta_{\tilde{\varepsilon}}(\eta x), \quad \tilde{\varepsilon} = \eta\varepsilon. \tag{18}$$

We take

$$\eta = \frac{1}{k}\sqrt{1 + k^2}, \tag{19}$$

where k is the slope of Γ as defined above. Using Eq. (18) the computed length of a straight line $\overline{S}_h$ (as given in Eq. (17)) is

$$\overline{S}_h = h\sum_{j_2\in\mathbb{Z}} \left(h\sum_{j_1\in\mathbb{Z}} \delta_\varepsilon(d(\Gamma, x_{j_1}, y_{j_2})) \right) = h\sum_{j_2\in\mathbb{Z}} \left(\eta h \sum_{j_1\in\mathbb{Z}} \delta_{\tilde{\varepsilon}}(\eta d(\Gamma, x_{j_1}, y_{j_2})) \right). \tag{20}$$

It can be verified from Fig. 2 that $\eta d(\Gamma, x_{j_1}, y_{j_2}) = x_{j_1} - x^*(y_{j_2})$ where

$$x^*(y_{j_2}) = x_n + ph, \quad 0 \leqslant p < 1, \quad n \in \mathbb{Z} \tag{21}$$

is the x-coordinate of Γ at $y = y_{j_2}$. Using the definition of the first discrete moment condition we can express $\overline{S}_h$ in terms of the first moment of $\delta_{\tilde{\varepsilon}}$ in the x-direction:

$$\overline{S}_h = h\sum_{j_2\in\mathbb{Z}} \left(\eta h \sum_{j_1\in\mathbb{Z}} \delta_{\tilde{\varepsilon}}(x_{j_1} - x^*(y_{j_2})) \right) = \eta h \sum_{j_2\in\mathbb{Z}} M_0(\delta_{\tilde{\varepsilon}}, x^*(y_{j_2}), h). \tag{22}$$

For the linear hat function $\delta_{\tilde{\varepsilon}}^L$ and the cosine approximation $\delta_{\tilde{\varepsilon}}^{\cos}$ with $\varepsilon = mh$ we have from Ref. [11] that

$$M_0\left(\delta_{mh}^L, x^*, h\right) = \frac{1}{m^2}\left((k_0 + k_1 + 1)m + (k_1 - k_0 - 1)p - \frac{k_0(k_0+1)}{2} - \frac{k_1(k_1+1)}{2} \right) \tag{23}$$

and

$$M_0\left(\delta_{mh}^{\cos}, x^*, h\right) = \frac{k_0 + k_1 + 1}{2m} + \frac{\sin((k_0 + k_1 + 1)\pi/2m)\cos(((k_1 - k_0)/2 - p)\pi/m)}{2m\sin(\pi/2m)}, \tag{24}$$

where

$$k_0 = \lfloor m - p \rfloor, \quad k_1 = \lfloor m + p \rfloor. \tag{25}$$

Here, $\lfloor m \rfloor$ denotes m rounded to the nearest integer towards minus infinity. We recall from Section 2.1 that one-dimensional delta function approximations are consistent if they fulfill the mass condition, i.e. $M_0(\delta_{mh}, x^*, h) = 1$ for any shift in the grid. The linear hat function with half width support $\varepsilon = mh$ satisfies the mass condition when m is an integer. The cosine

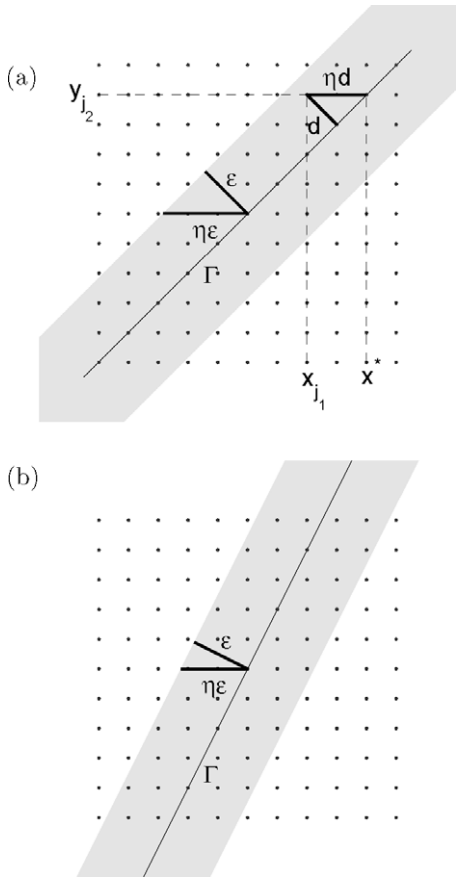

Fig. 2. Γ is a straight line with slope k, $\eta = \frac{1}{k}\sqrt{1+k^2}$, and $\varepsilon = 2h$. In (a) $k = 1, \eta = \sqrt{2}$, and x^*, defined in Eq. (21) is always a grid point, i.e. $p = 0$. In (b) $k = 2, \eta = \frac{\sqrt{5}}{2}$, and x^* is either a grid point or lies in the middle of two grid points, i.e. $p = 0$ and $p = 1/2$ every second time.

function with half width support $\varepsilon = mh$ satisfies the mass condition when $2m$ is an integer. In this case, when Γ is a straight line, the effective half width support is $\eta\varepsilon$ (see Fig. 2) and ηm and $2\eta m$, respectively, must be integers in order for the linear hat function and the cosine function to be consistent approximations.

Using Eq. (22) together with the formulas (23) and (24) we can evaluate the error in the computation of the length of a straight line with slope k using the linear hat function or the cosine approximation. The line in Fig. 2(a) has slope $k = 1$ and it intersects the grid points, hence $(x^*(y_{j_2}), y_{j_2})$ is always a grid point, i.e. $p = 0$. Using the delta approximation $\delta_\varepsilon = \delta_h^L$ as in [3] we get from Eqs. (22) and (23) with $\eta = \sqrt{2}, m = \eta$, and $p = 0$

$$\bar{S}_h = \frac{1}{2}(3\sqrt{2}-2)\sum_{j_2\in\mathbb{Z}}\sqrt{2}h = 1.1213\sum_{j_2\in\mathbb{Z}}\sqrt{2}h. \tag{26}$$

This indicates a relative error of over 12% independent of the mesh size h. This was also observed in [3]. With the delta approximation $\delta_\varepsilon = \delta_{2h}^{\cos}$ we get from Eqs. (22) and (24) with $\eta = \sqrt{2}, m = 2\eta$, and $p = 0$

$$\bar{S}_h = \frac{1}{2m}\left(5 + \frac{\sin(5\pi/(2m))}{\sin(\pi/(2m))}\right)\sum_{j_2\in\mathbb{Z}}\sqrt{2}h \approx 1.0035\sum_{j_2\in\mathbb{Z}}\sqrt{2}h. \tag{27}$$

This shows that a relative error of 0.35% independent of the mesh size h is expected when the approximation $\delta_{2h}^{\cos}$ is used. The line in Fig. 2(b) has slope $k = 2$ and it either intersect a grid point or lies in the middle of two grid points. Hence every second time $p = 1/2$ instead of $p = 0$. Thus, using $\delta_\varepsilon = \delta_h^L$ Eqs. (22) and (23) with $\eta = \frac{\sqrt{5}}{2}, m = \eta$ and $p = 0, p = 1/2$ every second time gives

$$\bar{S}_h = \left(\frac{3\sqrt{5}-4}{5} + \frac{2\sqrt{5}-2}{5}\right)\sum_{j_2\in\mathbb{Z}}\frac{\sqrt{5}}{2}h \approx 1.0361\sum_{j_2\in\mathbb{Z}}\frac{\sqrt{5}}{2}h. \tag{28}$$

This results in a relative error of 3.61% independent of mesh size. For $\delta_{2h}^{\cos}$ a relative error of around 0.013% is expected.

3.1. Numerical validation

In order to validate the results of the previous subsection we consider Γ being two parallel lines of length L at a normal distance $2a$, joined at both ends by a half circle with radius a. The slope of the lines to the x-axis is k. The length of Γ is $\overline{S} = 2L + 2\pi a$. Contours of the distance function $d(\Gamma, \mathbf{x})$ when $k = 2$ are shown in Fig. 3.

In Fig. 4(a) we show the relative error $E = |\overline{S}_h - \overline{S}|/\overline{S}$ where S_h is computed according to Eq. (17) with $\delta_\varepsilon = \delta_{2h}^{\cos}$ and $k = 1$. We can clearly see that there is no convergence as $h \to 0$. Eq. (27) indicates that the relative error for the straight lines is around 0.0035. We can see in the figure that this number is approached when the length of the straight lines is increased and the radius of the half circles is decreased.

In Fig. 4(b) the slope of the parallel lines is 2 and $\delta_\varepsilon = \delta_h^L$ has been used in the computation. There is no convergence. Eq. (28) indicates that the relative error for the straight lines is around 0.0361. We see in the figure that as the length of the straight lines is increased or the radius of the half circles is decreased the relative error approaches this number.

3.2. Mass condition reformulated using a Fourier transform

By the use of Poisson's summation formula

$$\alpha \sum_{j\in\mathbb{Z}} \varphi(\alpha j) = \sum_{j\in\mathbb{Z}} \hat{\varphi}(j/\alpha), \tag{29}$$

the mass condition for a regularized delta function $\delta_\varepsilon = \frac{1}{\varepsilon}\varphi(x/\varepsilon)$ with $\varepsilon = mh$ can be related to the Fourier transform of the function $\varphi(\xi)$

$$\hat{\varphi}(k) = \int_{-\infty}^{\infty} \varphi(\xi) e^{-2\pi i k\xi} d\xi, \tag{30}$$

in the following way:

$$M_0(\delta_{mh}, x^*, h) = \frac{1}{m} \sum_{j\in\mathbb{Z}} \varphi((j-p)/m) = \sum_{j\in\mathbb{Z}} e^{-2\pi i j p} \hat{\varphi}(jm). \tag{31}$$

The linear hat function, $\varphi^L(\xi)$, defined as in Eq. (4), has the Fourier transform

$$\hat{\varphi}^L(k) = \frac{\sin^2(\pi k)}{\pi^2 k^2}. \tag{32}$$

Thus, using Eq. (31) we have

$$M_0(\delta_\varepsilon^L, x^*, h) = 1 + \sum_{j\in\mathbb{Z}, j\neq 0} e^{-2\pi i j p} \left(\frac{\sin(\pi m j)}{\pi m j}\right)^2, \tag{33}$$

Here, we have used that $\hat{\varphi}^L(0) = 1$. The second term in Eq. (33) is zero independent of any shift in the grid x^* only when $\sin(\pi m j) = 0$ for all $j \in \mathbb{Z}, j \neq 0$. Therefore the mass condition is satisfied only for integers $m \geqslant 1$. This result can also be obtained using formula (23).

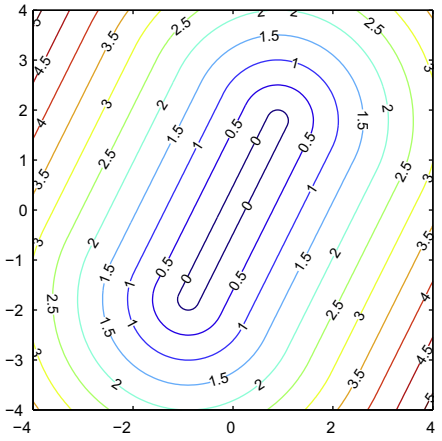

Fig. 3. Contours of the distance function $d(\Gamma, \mathbf{x})$. Γ is two parallel lines of length $L = 4$ at a normal distance $2a$, joined at both ends by a half circle of radius $a = 0.48/\sqrt{5}$. The slope of the lines to the x-axis is 2.

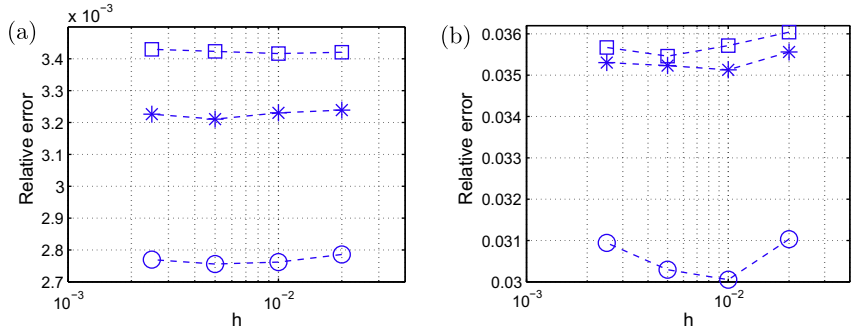

Fig. 4. The relative error $E = |\bar{S}_h - \bar{S}|/\bar{S}$ where Γ is two parallel lines of length L at a normal distance $2a$, joined at both ends by a half circle of radius a. In (a) the slope of the parallel lines is $k = 1$ and $\delta_\varepsilon = \delta_{2h}^{\cos}$ is used. Circles: $L = 4$, $a = 0.24\sqrt{2}$. Stars: $L = 6, a = 0.12\sqrt{2}$. Squares: $L = 6, a = 0.03\sqrt{2}$. The predicted relative error for the length of lines is around $3.5 \cdot 10^{-3}$. In (b) the slope of the parallel lines is $k = 2$ and $\delta_\varepsilon = \delta_h^L$ is used. Circles: $L = 4, a = 0.48/\sqrt{5}$. Stars: $L = 6, a = 0.12/\sqrt{5}$. Squares: $L = 6, a = 0.06\sqrt{2}$. The predicted relative error for the length of lines is around 0.0361.

The cosine approximation $\varphi^{\cos}(\xi)$, defined in Eq. (5), has the Fourier transform

$$\hat{\varphi}^{\cos}(k) = \begin{cases} \left(\frac{\sin(2\pi k)}{2\pi k}\right)\frac{1}{1-4k^2}, & \text{if } k \neq \pm 1/2, \\ 1/2, & \text{if } k = \pm 1/2. \end{cases} \tag{34}$$

By the same argument as above we have that the mass condition is satisfied only when $\sin(2\pi m j) = 0$ for all $j \in \mathbb{Z}, j \neq 0$ and $m \neq 1/2$. Therefore, the mass condition is satisfied when $m \geqslant 1$ and $2m$ is an integer.

In Eq. (22) we needed to evaluate $M_0(\delta_{\tilde{\varepsilon}}, x^*, h)$, where $\tilde{\varepsilon} = \eta m h$. From Poisson's summation formula we have

$$M_0(\delta_{\tilde{\varepsilon}}, x^*, h) = \sum_{j\in\mathbb{Z}} e^{-2\pi i j p}\hat{\varphi}(j\eta m). \tag{35}$$

Thus, in order to not have $\mathcal{O}(1)$ errors in the computation of the length of a straight line, m in $\varepsilon = mh$ must be chosen such that $\eta m \geqslant 1$ is an integer when $\delta_\varepsilon = \delta_\varepsilon^L$ and $\eta m \geqslant 1$, $2\eta m$ is an integer when $\delta_\varepsilon = \delta_\varepsilon^{\cos}$.

Remark. The regularized one-dimensional delta functions were in this section extended using the distance function. If instead a non-distance function $\phi(\mathbf{x})$ is used ε must be chosen differently in order to avoid $\mathcal{O}(1)$ errors. This is due to the fact that $\phi(\mathbf{x})$ does not give the physical distance, and hence a different scaling is needed.

Assume that $\hat{\varphi}(k)$ has compact support on $(-1, 1)$ and that $\hat{\varphi}(0) = 1$. Then, by Eq. (35), for all $m \geqslant 1/\eta$, the mass condition is satisfied. When $\phi(\mathbf{x})$ is a distance function we have that $\eta \geqslant 1$. This arises from the fact that the distance from Γ measured along a grid line is always larger or equal to the closest distance to Γ, which is given by the distance function, see Fig. 2. When $\eta \geqslant 1$ then for all $m \geqslant 1$, there is no $\mathcal{O}(1)$ error. If $\phi(\mathbf{x})$ is not a distance function and $|\nabla\phi| > 1$, a harder restriction on m is needed.

In the next section, we introduce a class of one-dimensional delta functions for which the $\hat{\varphi}(k)$ functions have compact support. We will see that this type of delta function approximations will satisfy the discrete moment conditions for a wide range of dilations.

4. Approximations with compact support in Fourier space

In the last section we saw that the linear hat function δ_ε^L and the cosine approximation $\delta_\varepsilon^{\cos}$ with $\varepsilon = mh$ are consistent approximations in one dimension only for a discrete set of m-values. Therefore they can lead to inconsistent approximations in higher dimensions. However, it is possible to construct delta function approximations that obey the mass condition for a wide range of dilations. We start by stating a theorem

Theorem 4.1. *Assume a regular grid in one dimension with grid points $x_j = jh, j \in \mathbb{Z}$ and let $x^* = x_n + ph$ where $0 \leqslant p < 1$ and $n \in \mathbb{Z}$. Consider a delta function approximation $\delta_\varepsilon = \frac{1}{\varepsilon}\varphi(x/\varepsilon)$ with $\varepsilon = mh$ where*

$$\varphi(\xi) = \int_{-\infty}^{\infty} \hat{\varphi}(k) e^{2\pi i k\xi} dk \tag{36}$$

and the Fourier transform of φ

$$\hat{\varphi}(k) = \int_{-\infty}^{\infty} \varphi(\xi) e^{-2\pi i k\xi} d\xi. \tag{37}$$

If $\hat{\varphi}(k)$ has compact support on $(-\beta, \beta)$ and

$$\left.\frac{\partial^r \hat{\varphi}(k)}{\partial k^r}\right|_{k=0} = \begin{cases} 1, & \text{for } r = 0, \\ 0, & \text{for } 1 \leqslant r < q. \end{cases} \tag{38}$$

Then for all $m \geqslant \beta$ the delta function approximation δ_ε satisfies q discrete moment conditions.

The discrete moment conditions are important for the accuracy of the one-dimensional delta function approximation, see Proposition 2.1. The conditions in Eq. (38) in the theorem are equivalent to the continuous moment conditions, i.e.

$$\left.\frac{\partial^r \hat{\varphi}(k)}{\partial k^r}\right|_{k=0} = \begin{cases} 1, & \text{for } r = 0, \\ 0, & \text{for } 1 \leqslant r < q \end{cases} \iff \int_{-\infty}^{\infty} \varphi(x) x^r dx = \begin{cases} 1, & \text{for } r = 0, \\ 0, & \text{for } 1 \leqslant r < q. \end{cases} \tag{39}$$

The continuous moment conditions will be important as we consider the analytical error in higher dimensions.

Proof of Theorem 4.1 There is no restriction in taking $n = 0$, such that $x^* = ph$, with $0 \leqslant p < 1$. Let $f_{r,\varepsilon}(x) = \frac{1}{\varepsilon}\varphi(x/\varepsilon)x^r$. We have

$$M_r(\delta_\varepsilon, x^*, h) = h\sum_{j\in\mathbb{Z}} \delta_\varepsilon(x_j - x^*)(x_j - x^*)^r = h\sum_{j\in\mathbb{Z}} \frac{1}{\varepsilon}\varphi((x_j - x^*)/\varepsilon)(x_j - x^*)^r = h\sum_{j\in\mathbb{Z}} f_{r,\varepsilon}((j-p)h). \tag{40}$$

Since the Fourier transform of $f_{r,\varepsilon}(x)$ is

$$\hat{f}_{r,\varepsilon}(k) = \frac{1}{(-2\pi i)^r}\frac{\partial^r}{\partial k^r}\hat{\varphi}(\varepsilon k) \tag{41}$$

and the Fourier transform of $f_{r,\varepsilon}(x - x^*)$ is $e^{-2\pi i k x^*}\hat{f}_{r,\varepsilon}(k)$ we have from Poisson's summation formula Eq. (29) that

$$M_r(\delta_\varepsilon, x^*, h) = \sum_{k\in\mathbb{Z}} e^{-2\pi i k p}\frac{1}{(-2\pi i)^r}\frac{\partial^r}{\partial k^r}\hat{\varphi}(\varepsilon k/h). \tag{42}$$

with $\varepsilon = mh$ we get

$$M_r(\delta_\varepsilon, x^*, h) = \frac{1}{(-2\pi i)^r}\left.\frac{\partial^r \hat{\varphi}(mk)}{\partial k^r}\right|_{k=0} + \frac{1}{(-2\pi i)^r}\sum_{k\in\mathbb{Z}, k\neq 0} e^{-2\pi i k p}\frac{\partial^r}{\partial k^r}\hat{\varphi}(mk). \tag{43}$$

If $\hat{\varphi}(k)$ has compact support in $(-\beta, \beta)$ the second term in the above equation vanishes for all $m \geqslant \beta$. Hence if the condition in Eq. (38) is satisfied for $r = 0, 1, \ldots, q-1$ then $\delta_\varepsilon = \frac{1}{\varepsilon}\varphi(x/\varepsilon)$ satisfies q discrete moment conditions. □

An example of a delta function approximation with the function $\hat{\varphi}(k)$ having compact support is the delta function introduced in Ref. [11]

$$\delta_\varepsilon^{TE}(x) = \frac{1}{\varepsilon}\varphi^{TE}(x/\varepsilon) \tag{44}$$

with

$$\varphi^{TE}(\xi) = \int_{-\infty}^{\infty} \hat{\varphi}^{TE}(k) e^{2\pi i k\xi} dk, \quad \hat{\varphi}^{TE}(k) = \begin{cases} e^{\frac{1}{d\beta^2}} e^{\frac{1}{d(k^2-\beta^2)}} & \text{if } |k| < \beta, \\ 0 & \text{if } |k| \geqslant \beta, \end{cases} \tag{45}$$

$d = 0.1$ and $\beta = 1$. Note that

$$\hat{\varphi}^{TE}(0) = 1, \quad \left.\frac{\partial \hat{\varphi}^{TE}(k)}{\partial k}\right|_{k=0} = 0, \quad \left.\frac{\partial^2 \hat{\varphi}^{TE}(k)}{\partial k^2}\right|_{k=0} = \frac{-2}{d\beta^4} \neq 0. \tag{46}$$

Hence from Theorem 4.1 we have that $\delta_{mh}^{TE}(x)$ is of moment order 2 for all $m \geqslant 1$. Thus, it is possible to construct one-dimensional delta function approximations that obey the discrete moment conditions for a wide range of dilations. These delta function approximations will not have compact support since they have compact support in Fourier space. However, if an approximation is decaying rapidly it can in practice be truncated.

It is computationally demanding to evaluate the approximation from its Fourier transform. Therefore, we would like to have an explicit expression for the approximation. In the following we give explicit expressions for two delta function approximations which have Fourier transforms that decay rapidly. Theorem 4.1 can then be used to find m-values for which $\delta_{mh}(x)$ satisfies the discrete moment conditions within a given error tolerance.

4.1. The derivative of the Fermi–Dirac function

Define a delta approximation as the derivative of the Fermi–Dirac or the sigmoid function

$$\delta_\varepsilon^{FD}(x) = \partial_x \frac{1}{1 + e^{-x/\varepsilon}} = \frac{1}{\varepsilon}\frac{e^{-x/\varepsilon}}{(1 + e^{-x/\varepsilon})^2}. \tag{47}$$

Let then $\delta_\varepsilon^{FD}(x) = \frac{1}{\varepsilon}\varphi^{FD}(x/\varepsilon)$, where

$$\varphi^{FD}(\xi) = \frac{e^{-\xi}}{(1+e^{-\xi})^2}. \tag{48}$$

The Fourier transform of $\varphi^{FD}(\xi)$ is

$$\hat{\varphi}^{FD}(k) = 1 - 4\pi k \Im\left(\sum_{j=1}^{\infty} \frac{(-1)^j}{j+2\pi i k}\right), \tag{49}$$

where $\Im$ represents the imaginary part. This was obtained by differentiating the Fourier transform of the Fermi–Dirac function given in Ref. [16]. We have

$$\hat{\varphi}^{FD}(0) = 1, \quad \left.\frac{\partial^r \hat{\varphi}^{FD}(k)}{\partial k^r}\right|_{k=0} = 0 \tag{50}$$

for r odd. However, the second derivative

$$\left.\frac{\partial^2 \hat{\varphi}^{FD}(k)}{\partial k^2}\right|_{k=0} = 16\pi^2\left(\sum_{j=1}^{\infty} \frac{(-1)^j}{j^2}\right) \neq 0. \tag{51}$$

Hence from Theorem 4.1 we have that $\delta^{FD}_{mh}(x)$ is of moment order 2 for all $m \geqslant \beta$ provided that $\hat{\varphi}^{FD}(k)$ has compact support in $(-\beta, \beta)$. Since $\hat{\varphi}^{FD}(k)$ does not have compact support, as was the case for $\hat{\varphi}^{TE}(k)$ we will always have a mass error but for $m = 2$ this error will be of order 10^{-16} which usually is the order of rounding errors. Therefore we consider $\hat{\varphi}^{FD}(k)$ to have compact support in (-2, 2) and thus by Theorem 4.1 $\delta^{FD}_{mh}(x)$ is of moment order 2 for all $m \geqslant 2$. In Fig. 5(b) (solid line) we can see that for $k = \pm 1$, $\hat{\varphi}^{FD}(k)$ is of order 10^{-7}. This implies that taking $m = 1$ will typically give a mass error that is of order 10^{-7}.

4.2. The Gaussian function

Another example of a function that has a Fourier transform that decays rapidly is the Gaussian function. The Fourier transform of a Gaussian is another Gaussian. Let

$$\varphi^{G}(\xi) = \sqrt{\frac{\pi}{9}} e^{-\pi^2 \xi^2/9}. \tag{52}$$

Then,

$$\hat{\varphi}^{G}(k) = e^{-9k^2}. \tag{53}$$

Also, for this function we have that

$$\hat{\varphi}^{G}(0) = 1, \quad \left.\frac{\partial^r \hat{\varphi}^{G}(k)}{\partial k^r}\right|_{k=0} = 0 \tag{54}$$

for all odd r but

$$\left.\frac{\partial^2 \hat{\varphi}^{G}(k)}{\partial k^2}\right|_{k=0} \neq 0. \tag{55}$$

Hence from Theorem 4.1 we have that $\delta^{G}_{mh}(x)$ is of moment order 2 for all $m \geqslant \beta$ provided that $\hat{\varphi}^{G}(k)$ has compact support in $(-\beta, \beta)$. Just as $\hat{\varphi}^{FD}(k)$, the function $\hat{\varphi}^{G}(k)$ is never zero. Therefore, it does not, strictly speaking, have compact support. However, since the function decreases exponentially to zero, it can in practice be regarded as zero whenever smaller than

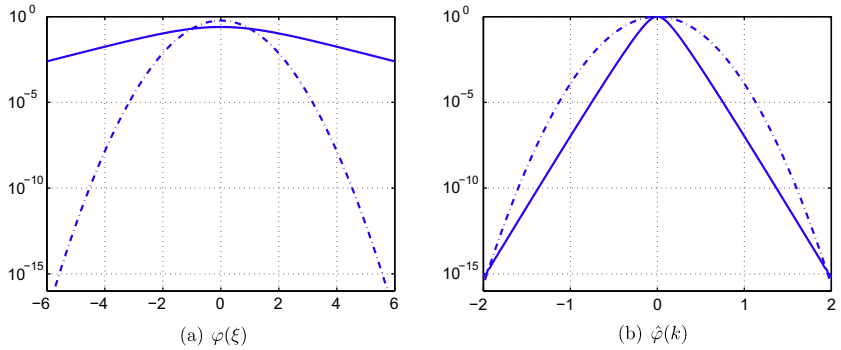

Fig. 5. The functions $\varphi(\xi)$ (a) used to define the regularized delta functions $\delta_\varepsilon(x) = \frac{1}{\varepsilon}\varphi(x/\varepsilon)$, and their Fourier transforms $\hat{\varphi}(k)$ (b). Solid lines: $\varphi(\xi) = \varphi^{FD}(\xi)$ and $\hat{\varphi}(k) = \hat{\varphi}^{FD}(k)$. Dash–dotted lines: $\varphi(\xi) = \varphi^{G}(\xi)$ and $\hat{\varphi}(k) = \hat{\varphi}^{G}(k)$.

some tolerance. In Fig. 5(b) we see the function $\hat{\varphi}^G(k)$ (dash–dotted line). For $k = \pm 1$, $\hat{\varphi}^G(k)$ is of order 10^{-5} and for $k = \pm 2$ it is of order 10^{-16} just as $\hat{\varphi}^{FD}(k)$. With an error tolerance of 10^{-16} we consider $\hat{\varphi}^G(k)$ to be of moment order 2 for all $m \geqslant 2$. We can see from Fig. 5(a) that the support of $\varphi^G(\xi)$ is much smaller than $\varphi^{FD}(\xi)$. Since, in practical computations, a narrow support of $\varphi(\xi)$ is desired the Gaussian approximation seems to be preferable.

In the next section we state and prove theorems about the error when the distance function is used to extend the one-dimensional delta approximations to higher dimensions.

5. Error analysis

Let Ω be the domain of integration. We assume throughout this section that the approximation $\delta_\varepsilon(d(\Gamma,\mathbf{x}))$ has compact support in

$$\Omega_\omega = \{\mathbf{x} : |d(\Gamma,\mathbf{x})| \leqslant \omega\}, \tag{56}$$

where $d(\Gamma,\mathbf{x})$ is the signed distance function and ω is small. We want to integrate

$$I_{\Gamma,F} = \int_\Omega \delta(d(\Gamma,\mathbf{x}))F(\mathbf{x})d\mathbf{x}. \tag{57}$$

The total error in the integration of the function $\delta(d(\Gamma,\mathbf{x}))F(\mathbf{x})$ approximated by $\delta_\varepsilon(d(\Gamma,\mathbf{x}))F(\mathbf{x})$ is

$$E_{tot,F}(\delta_\varepsilon) = \int_\Omega \delta(d(\Gamma,\mathbf{x}))F(\mathbf{x})d\mathbf{x} - \mathrm{quad}(\delta_\varepsilon(d(\Gamma,\mathbf{x}))F(\mathbf{x})), \tag{58}$$

where quad denotes the quadrature rule used to approximate the integral. The quadrature rule we consider is the trapezoidal rule. We split the total error into two parts: the analytical error made when replacing the integrand with its approximation

$$E_{\omega,F}(\delta_\varepsilon) = \int_{\Omega_\omega} \delta(d(\Gamma,\mathbf{x}))F(\mathbf{x})d\mathbf{x} - \int_{\Omega_\omega} \delta_\varepsilon(d(\Gamma,\mathbf{x}))F(\mathbf{x})d\mathbf{x} \tag{59}$$

and the numerical error made in the integration of this approximation using the trapezoidal rule

$$E_{\mathrm{quad},F}(\delta_\varepsilon) = \int_{\Omega_\omega} \delta_\varepsilon(d(\Gamma,\mathbf{x}))F(\mathbf{x})d\mathbf{x} - \mathrm{quad}(\delta_\varepsilon(d(\Gamma,\mathbf{x}))F(\mathbf{x})). \tag{60}$$

5.1. Analytical error

Definition 5.1. A function δ_ε with compact support in $[-\omega,\omega]$ satisfies α continuous moment conditions if

$$\int_{-\omega}^{\omega} \delta_\varepsilon(t)t^r dt = \begin{cases} 1, & \text{if } r = 0, \\ 0, & \text{if } 1 \leqslant r < \alpha. \end{cases} \tag{61}$$

We now state two theorems for the analytical error. The first theorem provides an expression for the analytical error in two dimensions, and the second theorem in three dimensions.

Theorem 5.1. *Let δ_ε be a continuous function with support in $[-\omega,\omega]$, $\omega = p\varepsilon$ that satisfies α continuous moment conditions, see Definition 5.1. Assume that Γ, the zero level set of $d(\Gamma,\mathbf{x})$, is a curve in $\mathbb{R}^2$ of class C^2 that can be parametrized by $\Gamma = (x(s),y(s)), x,y \in C^2[s1,s2]$ with the curvature $\kappa(s)$ defined by*

$$\kappa(s) = \frac{x'(s)y''(s) - x''(s)y'(s)}{q(s)^3}, \quad q(s) = \sqrt{x'(s)^2 + y'(s)^2} \neq 0. \tag{62}$$

Assume also that

$$\omega \max_s |\kappa(s)| < 1, \tag{63}$$

and that $F(\mathbf{x})$ is a smooth function. Then, the analytical error for the integration of $\delta(d(\Gamma,\mathbf{x}))F(\mathbf{x})$ made when replacing $\delta(d(\Gamma,\mathbf{x}))$ by $\delta_\varepsilon(d(\Gamma,\mathbf{x}))$ is given by

$$E_{\omega,F}(\delta_\varepsilon) = -\varepsilon^\alpha C_{\alpha,F} \int_{-p}^{p} \varphi(\xi)\xi^\alpha d\xi + \mathcal{O}(\varepsilon^{\alpha+1}), \tag{64}$$

with

$$C_{\alpha,F} = \frac{1}{\alpha!}\int_{s_1}^{s_2} q(s)f_{\alpha t}(s,0)ds - \frac{1}{(\alpha-1)!}\int_{s_1}^{s_2} q(s)\kappa(s)f_{(\alpha-1)t}(s,0)ds. \tag{65}$$

A proof of this theorem for $p = 1$ is given in Ref. [12] but a generalization is straightforward. The parametrization of $\Gamma = (x(s),y(s))$ and the normal vector of the curve defined by

$$\mathbf{n} = \frac{(-y'(s), x'(s))}{q(s)} \tag{66}$$

are used to parametrize the integration domain Ω_ω. Introducing the parametrization $X(s,t) = x(s) + tn^1(s)$, $Y(s,t) = y(s) + tn^2(s)$. The integration can be performed over $[s_1, s_2] \times [-\omega, \omega]$ when the condition in Eq. (63) is fulfilled. The function f in Eq. (65) is defined by

$$f(s,t) = F(X(s,t), Y(s,t)). \tag{67}$$

Theorem 5.2. *Let δ_ε be a continuous function with support in $[-\omega, \omega]$, $\omega = p\varepsilon$ that satisfies α continuous moment conditions, see Definition 5.1. Assume that Γ, the zero level set of $d(\Gamma, \mathbf{x})$, is a 2-manifold in $\mathbb{R}^3$ of class C^2. Suppose that $P^j(r,s) = (x(r,s), y(r,s), z(r,s)) : (r_1, r_2) \times (s_1, s_2) \to V_j$ is a coordinate patch on Γ of class C^2 and Γ is covered by the disjoint union of the open sets $V_1, \ldots, V_l$ and a set of measure zero in Γ. Let κ_1 and κ_2 be the principal curvatures of Γ on V_j. Assume also that*

$$\omega \max(\max_{r,s} |\kappa_1(r,s)|, \max_{r,s} |\kappa_2(r,s)|) < 1, \quad q(r,s) = \|P^j_r \times P^j_s\| \neq 0, \tag{68}$$

and that $F(\mathbf{x})$ is a smooth function. Then, the analytical error for the integration of $\delta(d(\Gamma, \mathbf{x}))F(\mathbf{x})$ made when replacing $\delta(d(\Gamma, \mathbf{x}))$ by $\delta_\varepsilon(d(\Gamma, \mathbf{x}))$ is given by

$$E_{\omega,F}(\delta_\varepsilon) = -\varepsilon^\alpha \int_{-p}^{p} \varphi(\xi)\xi^\alpha d\xi \sum_{j=1}^{l} C^j_{\alpha,F} + \mathcal{O}(\varepsilon^{\alpha+1}), \tag{69}$$

with

$$C^j_{1,F} = \int_{r_1}^{r_2} \int_{s_1}^{s_2} f_t(r,s,0) q(r,s) ds dr - \int_{r_1}^{r_2} \int_{s_1}^{s_2} f(r,s,0) q(r,s) (\kappa_1(r,s) + \kappa_2(r,s)) ds dr \tag{70}$$

and for $\alpha \geqslant 2$

$$\begin{aligned} C^j_{\alpha,F} = {} & \frac{1}{\alpha!} \int_{r_1}^{r_2} \int_{s_1}^{s_2} q(r,s) f_{\alpha t}(r,s,0) ds dr - \frac{1}{(\alpha-1)!} \int_{r_1}^{r_2} \int_{s_1}^{s_2} q(r,s)(\kappa_1(r,s) + \kappa_2(r,s)) f_{(\alpha-1)t}(r,s,0) ds dr \\ & + \frac{1}{(\alpha-2)!} \int_{r_1}^{r_2} \int_{s_1}^{s_2} q(r,s)(\kappa_1(r,s)\kappa_2(r,s)) f_{(\alpha-2)t}(r,s,0) ds dr. \end{aligned} \tag{71}$$

A proof can be found in the Appendix A. In order to perform the integration over Ω_ω we parametrize this region using the local parametrization of Γ and the normal vectors defined as

$$\mathbf{n} = (n^1, n^2, n^3) = \frac{1}{q(r,s)} (P^j_r \times P^j_s). \tag{72}$$

Introducing the parametrization $X^j(r,s,t) = x(r,s) + tn^1(r,s)$, $Y^j(r,s,t) = y(r,s) + tn^2(r,s)$, and $Z^j(r,s,t) = z(r,s) + tn^3(r,s)$ we can cover the domain Ω_ω by disjoint union of open sets $M_1, \ldots, M_l$ and a set of measure zero in Ω_ω, where

$$M_j = \{(x,y,z) : x = X^j(r,s,t), y = Y^j(r,s,t), z = Z^j(r,s,t), r \in (r_1, r_2), s \in (s_1, s_2), t \in [-\omega, \omega]\}. \tag{73}$$

The condition in Eq. (68) guarantees that this parametrization is non-singular. The integration can then be performed over $[r_1, r_2] \times [s_1, s_2] \times [-\omega, \omega]$. For ω small one can Taylor expand

$$f(r,s,t) = F(X^j(r,s,t), Y^j(r,s,t), Z^j(r,s,t)) \tag{74}$$

around $(r,s,0)$ and express the analytical error in terms of the continuous moments of the function δ_ε.

In the next section we analyze the numerical error made using the trapezoidal rule for integration.

5.2. Numerical error

The following theorem gives the error of the trapezoidal rule in one dimension.

Theorem 5.3. *Let*

$$x_n = a + nh, \quad n = 0, \ldots N, \quad h = \frac{b-a}{N} \tag{75}$$

be a decomposition of the interval $[a,b]$ and $T_h(a,b,h,\psi)$ be the trapezoidal sum

$$T_h(a,b,h,\psi) = h \sum_{n=0}^{N} w_n \psi(x_n), \tag{76}$$

where

$$w_n = \begin{cases} 1/2, & \text{for} \quad n = 0, \quad \text{and} \quad n = N, \\ 1, & \text{otherwise}. \end{cases} \tag{77}$$

Assume that $\psi(x) \in C^{2r+2}(a,b)$. *Then*

$$T_h - \int_a^b \psi(x)dx = R_T(a,b,h,\psi(x)) \tag{78}$$

with

$$R_T(a,b,h,\psi(x)) = \sum_{k=1}^{r} \frac{B_{2k}h^{2k}}{(2k)!}\psi^{2k-1}(x)\Big|_{x=a}^{b} + R_{2r+2}(a,b,h,\psi), \tag{79}$$

where B_j *are the Bernoulli numbers and* $R_{2r+2}(a,b,h,\psi)$ *is* $\mathcal{O}(h^{2r+2})$.

For a proof see Ref. [17, p. 298]. Note that when the function $\psi(x) \in C^\infty$ for $x \in \mathbb{R}$ and ψ has $[a,b]$ as an interval of periodicity, then

$$\psi^{(k)}(b) = \psi^{(k)}(a), \quad k = 0,1,2,\ldots. \tag{80}$$

Hence,

$$|R_T(a,b,h,\psi)| = \mathcal{O}(h^{2r+2}) \tag{81}$$

for arbitrary r. Therefore, we have that for periodic infinite differentiable functions the trapezoidal error tends to zero faster than any power of h, as $h \to 0$. This is referred to as superconvergence. In Ref. [18] another proof is given. It is shown by using the Poisson summation formula that the error

$$R_T = h\sum_{n=0}^{N} w_n\psi(x_n) - \int_a^b \psi(x)dx. \tag{82}$$

decreases as $\hat{\psi}(1/h)$, with

$$\hat{\psi}(k) = \int_{-\infty}^{\infty} \psi(x)e^{-2\pi ikx}dx. \tag{83}$$

If $\psi \in C^r[\mathbb{R}]$ and periodic, then $\hat{\psi}(1/h) = \mathcal{O}(h^r)$, as $h \to 0$. Thus, for $\psi \in C^\infty[\mathbb{R}]$ the trapezoidal rule converges faster than any power of h.

In higher dimensions we use the notion of a product rule. For simplicity we do the analysis here in two dimensions. The analysis in three dimensions is similar. Let $\Omega = [a,b] \times [c,d]$, and $\psi(x,y) \in C^{2r+2}(\Omega)$. Introduce a uniform grid

$$x_j = a + jh_x, \quad j = 0,\ldots M, \quad h_x = \frac{b-a}{M}, \quad y_n = c + nh_y, \quad n = 0,\ldots N, \quad h_y = \frac{d-c}{N}. \tag{84}$$

Denote by Q the quadrature scheme obtained by using the trapezoidal rule in both x and y directions with step size h_x and h_y. We can write

$$I = \int\int_\Omega \psi(x,y)dxdy = \int_c^d g(y)dy, \tag{85}$$

where

$$g(y) = \int_a^b \psi(x,y)dx. \tag{86}$$

Using the trapezoidal rule to integrate in the y-variable (see, Eqs. (76) and (77)) gives

$$I = h_y\sum_{n=0}^{N} w_n \int_a^b \psi(x,y_n)dx + R_T(c,d,h_y,g(y)), \tag{87}$$

where R_T is the quadrature error. Using also the trapezoidal method in the x-direction with step size h_x yields

$$I = h_y\sum_{n=0}^{N} w_n\left(h_x\sum_{j=0}^{M} w_j\psi(x_j,y_n) + R_T(a,b,h_x,\psi(x,y_n))\right) + R_T(c,d,h_y,g(y)). \tag{88}$$

Simplifying the expression we get

$$I = h_y h_x \sum_{n=0}^{N}\sum_{j=0}^{M} w_n w_j \psi(x_j, y_n) + \sum_{n=0}^{N} h_y w_n R_T(a, b, h_x, \psi(x, y_n)) + R_T\left(c, d, h_y, \int_a^b \psi(x, y)dx\right). \tag{89}$$

Hence

$$\left| I - h_y h_x \sum_{n=0}^{N}\sum_{j=0}^{M} w_n w_j \psi(x_j, y_n) \right| \leqslant (d-c) \max_{y_n} |R_T(a, b, h_x, \psi(x, y_n))| + (b-a) \max_{x\in[a,b]} \left|R_T\left(c, d, h_y, \psi(x, y)\right)\right|, \tag{90}$$

and we see that the convergence results from one dimension extend to two dimensions. Thus, the superconvergence of the trapezoidal rule also applies in two dimensions. We are now able to formulate the following theorem.

Theorem 5.4. *Let $\Omega = [a, b] \times [c, d]$, and Q be the quadrature scheme obtained by using the trapezoidal rule in both x and y directions with step size h_x and h_y. Suppose δ_ε has compact support in $[-\omega, \omega]$ and $\Omega_\omega \subset \Omega$ where*

$$\Omega_\omega = \{\mathbf{x} : |d(\Gamma, \mathbf{x})| \leqslant \omega\}. \tag{91}$$

Suppose further that $\delta_\varepsilon(d(\Gamma, \mathbf{x}))F(\mathbf{x}) \in C^\infty(\Omega)$. Then the numerical error

$$E_{Q,F}(\delta_\varepsilon) = \left| \int_\Omega \delta_\varepsilon(d(\Gamma, \mathbf{x}))F(\mathbf{x})d\mathbf{x} - Q(\delta_\varepsilon(d(\Gamma, \mathbf{x}))F(\mathbf{x})) \right| \tag{92}$$

decreases faster than any power of $h = \max(h_x, h_y)$.

When δ_ε has compact support in $[-\omega, \omega]$ the approximation $\delta_\varepsilon(d(\Gamma, \mathbf{x}))$ has compact support in Ω_ω. As long as $\Omega_\omega \subset \Omega$, $\delta_\varepsilon(d(\Gamma, \mathbf{x}))$ is a periodic function on Ω. Since the integrand is $C^\infty(\Omega)$ the superconvergence of the trapezoidal rule gives the result of the theorem.

The same result also holds in three dimensions.

5.3. Practical considerations

The theorems in the previous section are applicable to delta function approximations with compact support in $[-\omega, \omega]$. The delta function approximations presented in Section 4 are infinitely differentiable and satisfy two moment conditions but do not have compact support. In practice, we will truncate the delta function approximations presented in Section 4 and set them to zero outside some $[-\omega, \omega]$ interval. This is motivated by the fact that the delta function approximations δ_ε in question decay exponentially fast. The truncation results in an approximation error. In the following, we comment on the error we make by truncating the tail of δ_ε^{FD} and δ_ε^{G} and discuss how the theorems in the previous section can be used.

Denote the truncated delta function approximation by

$$\delta_\varepsilon^\omega(t) = \begin{cases} \delta_\varepsilon(t), & \text{for } t \text{ in } [-\omega, \omega], \\ 0, & \text{otherwise}, \end{cases} \tag{93}$$

where $\delta_\varepsilon(t)$ is one of the one-dimensional delta function approximations presented in Section 4 and ω is the half width support of the truncated delta function.

In two and three dimensions, we split the total error in the integration of the function $\delta(d(\Gamma, \mathbf{x}))F(\mathbf{x})$ approximated by $\delta_\varepsilon^\omega(d(\Gamma, \mathbf{x}))F(\mathbf{x})$ into two parts: the analytical error $E_{\omega,F}(\delta_\varepsilon^\omega)$ defined in Eq. (59) and the numerical error $E_{\text{quad},F}(\delta_\varepsilon^\omega)$ defined in Eq. (60). The analytical error in two dimensions is given by Theorem 5.1 and in three dimensions by Theorem 5.2. This error depends on the number of continuous moment conditions the delta function approximation satisfies. All the delta function approximations δ_ε in Section 4 satisfy two continuous moment conditions, see Eq. (39). By truncating these delta function approximations we make an approximation error and the continuous moment conditions are only satisfied to a certain level of accuracy depending on the truncation parameter ω.

In the following, we estimate the error we make by truncating the tail of δ_ε. In two dimensions the analytical error for the truncated approximation $\delta_\varepsilon^\omega$ is

$$E_{\omega,F}(\delta_\varepsilon^\omega) = \left(1 - \int_{-\omega}^{\omega} \delta_\varepsilon^\omega(t)dt\right) \int_{s_1}^{s_2} q(s)f(s, 0)ds - C_{1,F} \int_{-\omega}^{\omega} \delta_\varepsilon^\omega(t)tdt + \mathcal{O}(\varepsilon^2), \tag{94}$$

where $C_{1,F}, q(s)$, and $f(s, t)$ are all defined in Theorem 5.1. Note that the only difference in three dimensions are the constants in front of the one-dimensional continuous moment conditions, see Theorem 5.2.

Since both δ_ε^{FD} and δ_ε^{G} are even functions we have that

$$\int_{-\infty}^{-\omega} \delta_\varepsilon(t)tdt + \int_{\omega}^{\infty} \delta_\varepsilon(t)tdt = 0. \tag{95}$$

From the definition of $\delta_\varepsilon^\omega$, Eq. (93) and since both δ_ε^{FD} and δ_ε^{G} satisfy the second continuous moment condition, i.e.

$$\int_{-\infty}^{\infty} \delta_\varepsilon(t)tdt = \int_{-\omega}^{\omega} \delta_\varepsilon(t)tdt + \int_{-\infty}^{-\omega} \delta_\varepsilon(t)tdt + \int_{\omega}^{\infty} \delta_\varepsilon(t)tdt = 0, \tag{96}$$

the compactly supported delta function approximations also satisfy the second moment condition and hence the second term in Eq. (94) is zero. To estimate the first term in Eq. (94) we need to estimate

$$I_1 = \int_{\omega}^{\infty} \delta_\varepsilon(t) f(t) dt \tag{97}$$

and

$$I_2 = \int_{-\infty}^{\omega} \delta_\varepsilon(t) f(t) dt. \tag{98}$$

For $\delta_\varepsilon = \delta_\varepsilon^{FD}(t)$ we have

$$|I_1^{FD} + I_2^{FD}| = \frac{2}{1 + e^{\omega/\varepsilon}} \tag{99}$$

and for $\delta_\varepsilon = \delta_\varepsilon^{G}(t)$

$$|I_1^{G} + I_2^{G}| = 1 - \operatorname{erf}\left(\frac{\pi\omega}{3\varepsilon}\right), \tag{100}$$

where erf is the error function defined by

$$\operatorname{erf}(x) = \frac{2}{\sqrt{\pi}} \int_0^x e^{-t^2} dt. \tag{101}$$

Thus, given a tolerance one can choose ω/ε such that $|I_1 + I_2|$ is below the given tolerance. Then, the analytical error is $\mathcal{O}(\varepsilon^2)$ down to the given tolerance.

The analysis of the numerical error in two and three dimensions presented in Section 5.2 is based on the superconvergence of the trapezoidal rule for periodic infinitely differentiable functions. By truncating the delta function approximations presented in Section 4 we make an approximation error and a mismatch in the odd derivatives at $\pm\omega$, i.e. $\varphi^{2k-1}(\omega) \neq \varphi^{2k-1}(-\omega)$ results in an error, see Theorem 5.3. However, if the function φ is very small when truncated we expect the error in the trapezoidal rule to be small.

The total error is hence a sum of the analytical and the numerical error. We suggest here a way to select ε and the half width support ω so that the delta function approximations with compact support are second-order accurate down to a specified error tolerance. We have seen in numerical experiments that choosing ω and ε according to this algorithm gives a total error below the given tolerance. Given a tolerance C, appropriate values for ε and ω can be determined by the following steps:

1. choose the smallest β such that $\hat{\varphi}(\beta) < C$,
2. let $\varepsilon = mh$ and take $m = \beta$, then
3. for this ε choose ω such that
4. $\delta_\varepsilon(\omega) \leqslant C$.

In the first step we want to get a one-dimensional delta function approximation δ_{mh} that satisfies two discrete moment conditions down to the specified error tolerance C for all $m \geqslant \beta$. In the second step we choose the smallest such m and in the third step we truncate the delta function within the same accuracy. In Figs. 6 and 7 we show the chosen m and ω/h for

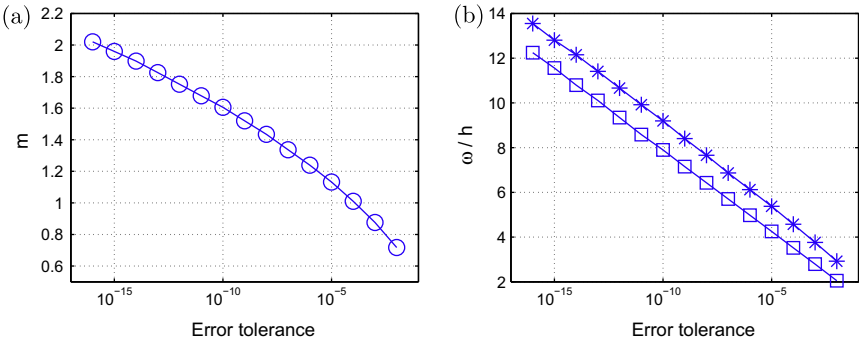

Fig. 6. For the delta function δ_{mh}^G we show in (a) m as a function of error tolerance. We show the smallest m such that $\hat{\varphi}^G(m)$ is below the given error tolerance. In (b) we show the half width support of δ_{mh}^G divided by h when m from (a) is used. The support is computed with the same error tolerance that was used to find the appropriate m-value. This calculation was made for two different values of $h, h = 10^{-6}$ (stars) and $h = 10^{-2}$ (squares) and gives an idea of where the delta function approximation can be truncated. For a tolerance of 10^{-6} the optimal m is, for example, around 1.25 and the half width support is around $6h$, while for a requested tolerance of $10^{-16}, m \approx 2$ and the half width support is around $14h$.

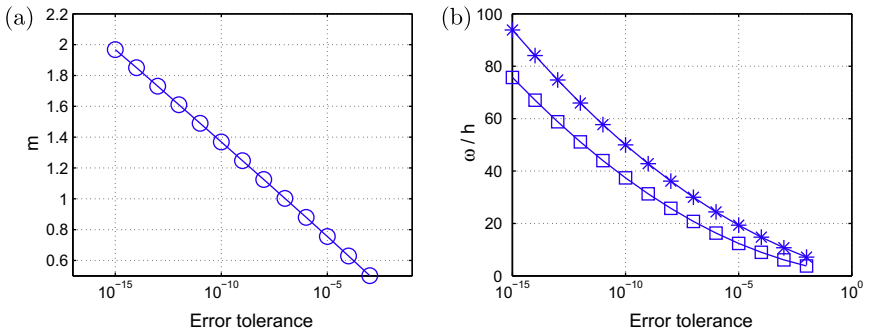

Fig. 7. The delta function δ^{FD}_{mh} is used. This figure should be compared with Fig. 6. In (a) we show the smallest m such that $\hat{\varphi}^G(m)$ is below the given error tolerance. In (b) we show the half width support divided by h of δ^{FD}_{mh} when m from (a) is used. The support is computed with the same error tolerance that was used to find the appropriate m-value. This calculation was made for two different values of h, $h = 10^{-6}$ (stars) and $h = 10^{-2}$ (squares) and gives an idea of where the delta function approximation can be truncated. Here, for a tolerance of 10^{-6} the optimal m is somewhat smaller than 1. The half width support of the delta function approximation is around $22h$. Note that this is much larger than the half width support of the Gaussian approximation which is around $6h$ for the same tolerance, see Fig. 6.

different error tolerances for δ^G_ε and δ^{FD}_ε, respectively. As an example, consider a tolerance of $C = 10^{-6}$. For this tolerance, the optimal m for the Gaussian approximation is around 1.25 and the half width support ω is around $6h$. For the derivative of the Fermi–Dirac function, the optimal m is around 0.9 and the half width support $\omega = 22h$. The widths for the different functions are in agreement with their decay behaviors, see Fig. 5. The Gaussian function decays much faster than the derivative of the Fermi–Dirac function. The difference between the half width support ω of the Gaussian approximation and the derivative of the Fermi–Dirac function is larger for smaller error tolerances. In practical computations the Gaussian function is preferable.

6. Numerical results

In this section, we present three numerical examples using the distance function to extend the one-dimensional regularized delta functions $\delta^{FD}_\varepsilon, \delta^G_\varepsilon$, and δ^{TE}_ε to higher dimensions. We also show results when non-distance functions are used. Here, we study the rate of convergence numerically by mesh refinement. In all the examples in this section we have integrands with non-vanishing second derivatives and $\varepsilon = mh$. Since the approximations $\delta^{TE}_\varepsilon, \delta^{FD}_\varepsilon$, and δ^G_ε all are of continuous moment order 2, we expect to have an analytical error of $\mathcal{O}(h)^2$ in both two and three dimensions, according to Theorems 5.1 and 5.2.

Example 1. Consider the problem of computing the line integral

$$I = \int_\Gamma 3x^2 - y^2 ds = 2\pi, \tag{102}$$

where Γ is a circle of radius 1 centered at the origin. This problem has previously been considered by Smereka, see Table 3 in Ref. [7]. We cover the domain $\Omega = \{\mathbf{x} = (x,y) : |x| \leqslant 2, |y| \leqslant 2\}$ with a regular grid

$$x_i = -2 + ih, \quad i \in \mathbb{Z}, \tag{103}$$
$$y_j = -2 + jh, \quad j \in \mathbb{Z}, \tag{104}$$

and approximate the line integral I by

$$I_h = h^2 \sum_{j\in\mathbb{Z}} \sum_{i\in\mathbb{Z}} \left(3x_i^2 - y_j^2\right) \delta^{FD}_{mh}(\phi(\Gamma,(x_i,y_j))). \tag{105}$$

In Fig. 8 the relative error $E = |I_h - I|/I$ is shown for $m = 1$, 2, and 2.5. In Fig. 8(a) the level set function $\phi(\Gamma,\mathbf{x}) = d(\Gamma,\mathbf{x})$ and we see second-order convergence. The mass error in the case when $m = 1$ is of order 10^{-7} (see Fig. 6) and cannot be seen in the plot. We have also used the level set function $\phi(\Gamma,\mathbf{x}) = x^2 + y^2 - 1$ as in Ref. [7], which is not a signed distance function. The results are shown in Fig. 8(b) and indicate second-order convergence for $m \geqslant 2$. In the case of this non-distance function the mass error increases as expected (see the Remark in Section 3). For $m = 1$ the curve representing the error (circles in Fig. 8(b)) flattens out as h decreases since the total error is then dominated by the mass error.

Example 2. Here, we consider the computation of the surface integral:

$$I = \int_\Gamma (4 - 3x^2 + 2y^2 - z^2) dA = \frac{40\pi}{3}, \tag{106}$$

where Γ is a sphere of radius 1 centered at the origin. In Refs. [7,9] the level set function $u(\Gamma,\mathbf{x}) = x^2 + y^2 + z^2 - 1$ is used to extend one-dimensional regularized delta functions to three dimensions. The relative error using $\delta^{FD}_{2h}(u(\Gamma,\mathbf{x}))$ and $\delta^G_{2h}(u(\Gamma,\mathbf{x}))$

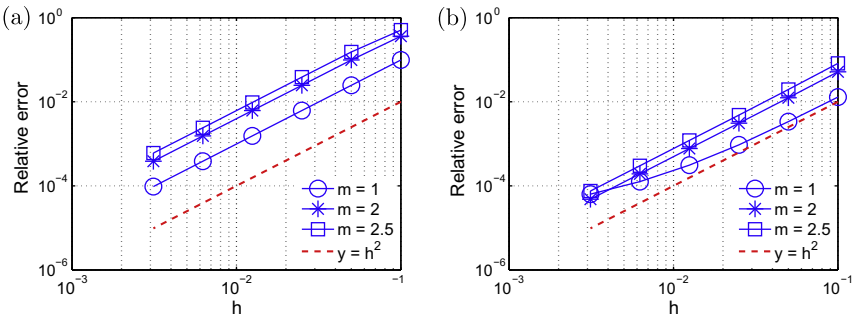

Fig. 8. The relative error $E = |I_h - I|/I$ where I and I_h are defined in Eqs. (102) and (105), respectively. We have used δ^{FD}_{mh} with $m = 1$ (circles), $m = 2$ (stars), and $m = 2.5$ (squares). The dashed line is $y = h^2$. In (a) the level function is the signed distance function. In (b) the level function $\phi(\Gamma, \mathbf{x}) = x^2 + y^2 - 1$ is used.

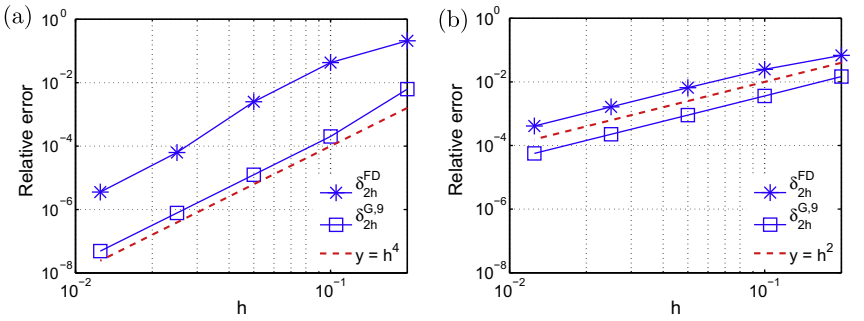

Fig. 9. The relative error in the computation of the surface integral in Eq. (106) when Γ is a sphere of radius 1 centered at the origin. The results are for $\delta^{FD}_{2h}(u(\Gamma, \mathbf{x}))$ (stars) and $\delta^{G}_{2h}(u(\Gamma, \mathbf{x}))$ (squares). In (a) the level function is the signed distance function. In (b) the level function $u(\Gamma, \mathbf{x}) = x^2 + y^2 + z^2 - 1$ is used.

is shown in Fig. 9(b), where second-order convergence can be seen. In Fig. 9(a) we use the distance function and observe that the convergence is faster than second-order. Using spherical coordinates to parametrize the sphere Γ one can show that the constant $C_{2,F}$ in the analytical error defined in Theorem 5.2 (Eq. (71)) with $F = 4 - 3x^2 + 2y^2 - z^2$ is zero. Further, since both delta approximations used here satisfy all the odd moment conditions, the convergence is of fourth-order, in accordance with Theorem 5.2. The results are similar when the center of the sphere is shifted. The relative error is smaller when $\delta^{G}_{2h}(u(\Gamma, \mathbf{x}))$ is used compared to $\delta^{FD}_{2h}(u(\Gamma, \mathbf{x}))$. This is also in accordance with Theorem 5.2 since the width ω of δ^{G}_{2h} is much smaller than the width of δ^{FD}_{2h} (see Section 5.3). Consequently, the constant in the analytical error is smaller.

6.1. Partial differential equations

We consider now the differential equation,

$$Lu = \delta(\Gamma, g, \mathbf{x}), \quad \mathbf{x} \in \Omega \subset \mathbb{R}^d, \quad Bu = r(\mathbf{x}), \quad \mathbf{x} \in \partial\Omega. \tag{107}$$

The solution can be written as

$$u(\mathbf{x}) = \int_\Omega G(\mathbf{x}, \mathbf{y}) \delta(\Gamma, g, \mathbf{y}) d\mathbf{y} + R(\mathbf{x}), \tag{108}$$

where $G(\mathbf{x}, \mathbf{y})$ is Green's function and $R(\mathbf{x})$ represents the contribution from the boundary conditions. In the case of homogeneous boundary conditions $R(\mathbf{x}) = 0$. In the computations the delta function is approximated by a regularized delta function $\delta_\varepsilon(\Gamma, g, \mathbf{x})$ with support in the interval $[-\omega, \omega]$. Assume that Green's function $G(\mathbf{x}, \mathbf{y})$ is regular away from $\mathbf{x} = \mathbf{y}$ for all $\mathbf{y} \in \Gamma$. Then, for all $\mathbf{x}_j$ for which $|\mathbf{x}_j - \mathbf{x}| > \omega$ for all $\mathbf{x} \in \Gamma$,

$$|u_j - u(\mathbf{x}_j)| \leqslant Ch^{\min(p,q)}, \tag{109}$$

where q is the order of accuracy of the delta function approximation and p is the order of accuracy for the discretization of the differential operator L. For a proof see Ref. [3].

Example 3. Let us consider the Poisson equation in $\mathbb{R}^2$

$$-\Delta u = \delta(\Gamma,\mathbf{x}), \quad \mathbf{x}\in\Omega\subset\mathbb{R}^2 \quad u(\mathbf{x}) = v(\mathbf{x}), \quad \mathbf{x}\in\partial\Omega \tag{110}$$

where $\Omega = \{\mathbf{x} = (x^{(1)},x^{(2)}) : \ |x^{(1)}| \leqslant 1, |x^{(2)}| \leqslant 1\}$, $\Gamma = \{\mathbf{x} : |\mathbf{x}-\hat{\mathbf{x}}| = 1/2\}$, and $v(\mathbf{x}) = 1 - \log(2|\mathbf{x}-\hat{\mathbf{x}}|)/2$. The solution of this equation is

$$u(\mathbf{x}) = \begin{cases} 1 & |\mathbf{x}-\hat{\mathbf{x}}| \leqslant 1/2, \\ 1-\log(2|\mathbf{x}-\hat{\mathbf{x}}|)/2, & |\mathbf{x}-\hat{\mathbf{x}}| > 1/2, \end{cases} \tag{111}$$

see Fig. 10. We introduce a uniform grid, with step size $h = 2/N$ in both $x^{(1)}$ and $x^{(2)}$ direction. The delta function approximations δ_ε^{FD}, δ_ε^{G}, δ_ε^{TE}, and δ_ε^{C} are tested for $\varepsilon = mh$. We use a fourth-order stencil D_2^4 to approximate the differential operator. See [3] for the definition of D_2^4. The error,

$$\|u-u_h\|, \tag{112}$$

is measured in both the maximum norm and the L1-norm. Here, u is the exact solution given in Eq. (111) and u_h is the numerical solution. In Figs. 11 and 12 we show the error when the circle Γ is centered in $\hat{x} = (0,0)$. In Fig. 11 the maximum norm measured over the whole domain Ω when δ_{mh}^{FD} and δ_{mh}^{G} are used is shown for $m = 1$, $m = 2$, and $m = 3$. We have first-order convergence since we measured the error close to Γ. To measure the error away from Γ, we introduce the sub-domain

$$\widetilde{\Omega} = \{\mathbf{x} : \mathbf{x}\in\Omega, \ |d(\Gamma,\mathbf{x})| > \eta\}. \tag{113}$$

Since $\delta_\varepsilon^{FD}, \delta_\varepsilon^{G}$, and δ_ε^{TE} are all second-order accurate we expect from Eq. (109) to see second-order convergence when the error is measured away from Γ. We recall that analytical results suggested that $\eta \geqslant \omega$ is needed to obtain the convergence order of the delta function approximation, see Eq. (109). However, our numerical simulations indicate that $\eta = \varepsilon$ is sufficient. In Fig. 12 the maximum norm and the L1-norm of the error is shown for $\delta_{2h}^{FD}, \delta_{2h}^{G}, \delta_{2h}^{TE}$, and δ_{2h}^{C}. For the regularized delta function δ_{2h}^{C} of order h^4 in one dimension there is no convergence, neither in the maximum norm nor in the L1-norm. Note that the error using δ_{2h}^{G} is almost identical to the error we obtain using δ_{2h}^{TE}.

We obtained similar results for other values of $\hat{x}$ away from the boundary of the computational domain.

7. Conclusions

We have introduced delta function approximations that are convenient to use for delta functions with support on a curve in 2D or a surface in 3D, represented implicitly by a level set. The framework is based on the "old" method with a one-dimensional delta function approximation extended to higher dimensions by a distance function.

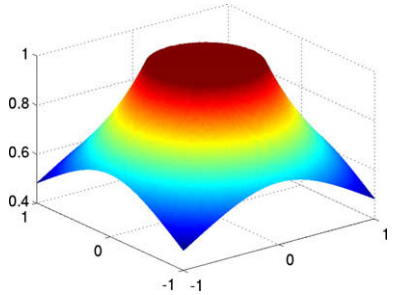

Fig. 10. The exact solution $u(\mathbf{x})$ given by Eq. (111) for $\hat{\mathbf{x}} = 0$.

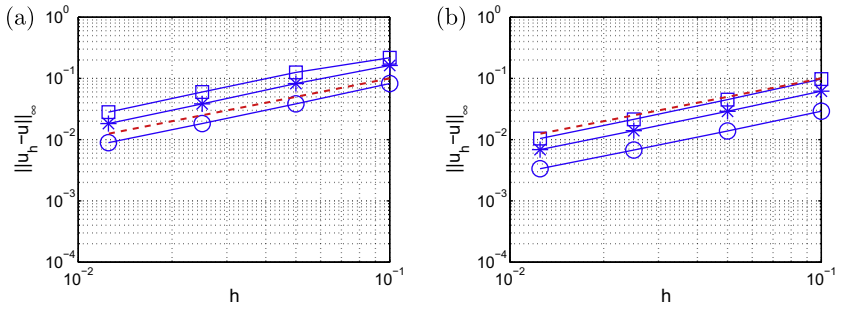

Fig. 11. The maximum norm of the error measured over Ω is shown for δ_{mh}, $m = 1$ (circles), $m = 2$ (stars), and $m = 3$ (squares). A fourth-order discretization for the differential operator has been used. The dashed line is $y = h$. In (a) $\delta_{mh} = \delta_{mh}^{FD}$ is used. In (b) $\delta_{mh} = \delta_{mh}^{G}$ is used. As expected, we see a first-order error, since we have measured the error also close to Γ.

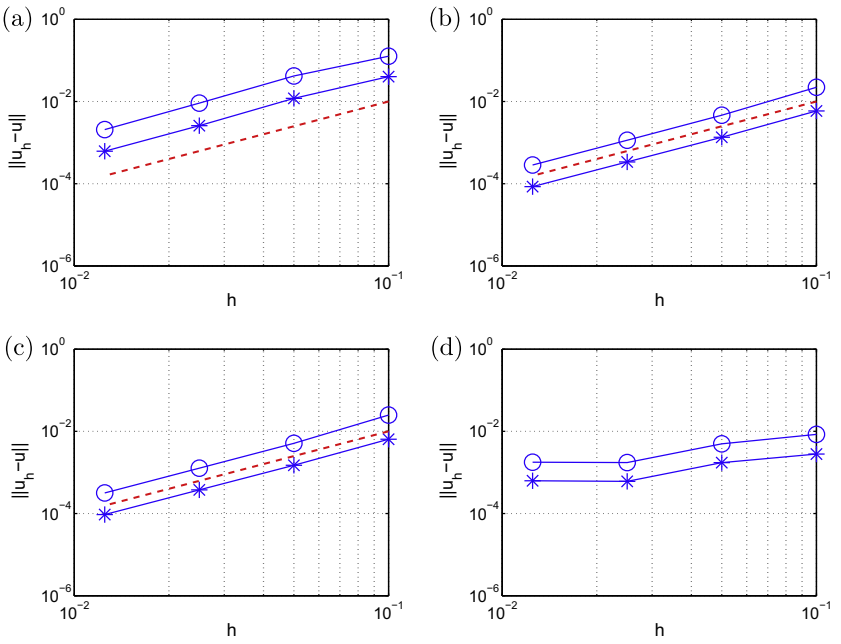

Fig. 12. The error measured over $\widetilde{\Omega}$ (this domain is defined in (113) with $\eta = 0.2$) using a fourth-order discretization of the differential operator. The max-norm of the error (circles) and the L1-norm (stars) are shown. The dashed line is $y = h^2$. In (a) $\delta_\varepsilon = \delta_{2h}^{FD}$. In (b) $\delta_\varepsilon = \delta_{2h}^{G}$. In (c) $\delta_\varepsilon = \delta_{2h}^{TE}$. In (d) $\delta_\varepsilon = \delta_{2h}^{C}$. The second-order convergence is now obtained in (a)–(c), as we are excluding the region closest to Γ, as explained in the text.

This method was in [3] shown to be inconsistent when different compact one-dimensional delta function approximations were used. In this paper, we have shown that this can be understood from the fact that these compact functions cannot both satisfy the discrete mass condition for all shifts in the grid *and* for a range of dilations of the support. This is however possible if one is basing the approximation on functions that have compact support instead in Fourier space, or in practice, that are smaller than some tolerance outside a given interval. For such functions, we have proven in both two and three dimensions that the error can be bounded by the sum of the analytical and the numerical error. The analytical error is determined by the moment order of the one-dimensional approximation and the numerical error tends to zero faster than any power of h in the limit as $h \to 0$, due to the superconvergence of the trapezoidal rule. All the three functions we have discussed have analytical errors of $\mathcal{O}(h^2)$. When we are to compute an integral over the delta function itself, yielding length of curve or surface area, or over the delta function multiplied by a linear function, there is no analytical error for any of the approximations that we have introduced, since the approximate delta functions are of moment order 2.

A function that is compact or decays rapidly in Fourier space will not produce delta function approximations with compact support. This means that in practice, we need to truncate these approximations. For the Gaussian function δ_ε^G, that was introduced in Section 4.2, the accuracy of this procedure was discussed in conjunction with Fig. 6 in Section 5.3. It was concluded that to achieve an error around 10^{-6} we need $\varepsilon \geqslant mh, m = 1.25$. For $m = 1.25$ the Gaussian function can be truncated so that the half width support becomes around $6h$. To get an error around 10^{-16}, we need $m = 2$ and a half width support of around $14h$. When we have non-vanishing second derivatives of the function F, see (57), there will be an analytical error of $\mathcal{O}(h^2)$ which will dominate the numerical error, and for moderate grid sizes, there is no point in using a wider support than $6h$.

In this paper, we also discussed the function δ_ε^{TE}, as defined in (44). This function yields very similar results to the Gaussian, but is more computationally expensive, since the function is not given explicitly but must be computed from its Fourier transform. We found that, compared to the other approximations, the approximation δ_ε^{FD}, has a slower decay in real space and hence a larger support. We therefore recommend to use the Gaussian approximation.

Acknowledgment

S.Z. thanks Gunilla Kreiss and Emanuel Rubensson for valuable comments and helpful discussions during the preparation of the manuscript.

A.-K.T. acknowledges the support she has received from the Knut and Alice Wallenberg Foundation as a Royal Swedish Academy of Science Fellow.

Appendix A. We start by stating a definition and a theorem from Ref. [19] that will be used in the study of the analytical error in three dimensions.

Definition 8.1. Let $k > 0$. A k-manifold in $\mathbb{R}^n$ of class C^r is a subspace M of $\mathbb{R}^n$ having the following property: For each $p \in M$, there is an open set V of M containing p, a set U that is open in either $\mathbb{R}^k$ or the upper half-space in $\mathbb{R}^k$ and a continuous map $P : U \to V$ carrying U onto V in one-to-one fashion, such that:

1. P is of class C^r.
2. $P^{-1} : V \to U$ is continuous.
3. $DP(\mathbf{x})$, the Jacobian matrix of P, has rank k for each $\mathbf{x} \in U$.

The map P is called a coordinate patch on M about p.

Theorem 8.1. *Let M be a compact k-manifold in $\mathbb{R}^n$, of class C^r. Let $f : M \to \mathbb{R}$ be a continuous function. Suppose that $P_i : A_i \to M_i$, for $i = 1, \ldots, N$ is a coordinate patch on M, such that A_i is open in $\mathbb{R}^k$ and M is the disjoint union of the open sets $M_1, \ldots, M_N$ of M and a set K of measure zero in M. Then*

$$\int_M f dV = \sum_{i=1}^{N} \int_{A_i} (f \circ P_i) V(DP_i). \tag{114}$$

This theorem states that $\int_M f dV$ can be evaluated by separately evaluating the integral over local parametrized parts of the manifold and then summing up all the contributions. A proof of the theorem can be found in Ref. [19]. It is assumed that the support of the integrand f lies in M.

Proof of Theorem 5.2. In three dimensions we cannot expect to have a global parametrization but a local exist. By the assumption Γ is a 2-manifold that can be covered by an union of disjoint open sets $V_1, \ldots, V_l$ and a set K of measure zero in Γ. It has been proven that such sets can be constructed using polygonal charts sets, see [20]. Further, we have assumed that a coordinate patch $P^j = (x(r,s), y(r,s), z(r,s)) : (r_1, r_2) \times (s_1, s_2) \to V_j$ of class C^2 on Γ exists.

The normal of Γ at V_j is defined as $\mathbf{n} = (n^1, n^2, n^3) = \frac{1}{q(r,s)}(P^j_r \times P^j_s)$, where $q(r,s) = \|P^j_r \times P^j_s\| \neq 0$.

The integration is over Ω_ω. This is a compact 3-manifold of class C^2. The integrand $\delta_\varepsilon F : \Omega_\omega \to \mathbb{R}$, is a continuous function. The domain Ω_ω can be covered by the disjoint union of open sets $M_1, \ldots, M_l$ and a set of measure zero in Ω_ω. The open set M_j can be given by the following parametrization

$$M_j = \{(x,y,z) : x = X^j(r,s,t),\ y = Y^j(r,s,t), z = Z^j(r,s,t), \quad r \in (r_1, r_2), s \in (s_1, s_2), t \in [-\omega, \omega]\}, \tag{115}$$

where $X^j(r,s,t) = x(r,s) + tn^1(r,s), Y^j(r,s,t) = y(r,s) + tn^2(r,s)$, and $Z^j(r,s,t) = z(r,s) + tn^3(r,s)$. Let $A_j = (r_1, r_2) \times (s_1, s_2) \times [-\omega, \omega]$, and

$$\beta^j = (X^j(r,s,t), \quad Y^j(r,s,t), \quad Z^j(r,s,t)). \tag{116}$$

Then it follows from Theorem 8.1 that:

$$I_{\Omega_\omega}(\delta_\varepsilon F) = \sum_{j=1}^{l} I_{A_j} = \sum_{j=1}^{l} \int_{A_j} (\delta_\varepsilon \circ \beta^j)(F \circ \beta^j) V(D\beta^j), \tag{117}$$

where $V(D\beta^j) = |\det(J(r,s,t))| dt ds dr$. The Jacobian determinant for this transformation from (x,y,z) to (r,s,t) is

$$\begin{aligned} \det(J(r,s,t)) &= (X^j_r, Y^j_r, Z^j_r) \times (X^j_s, Y^j_s, Z^j_s) \cdot (X^j_t, Y^j_t, Z^j_t) = (P^j_r \times P^j_s + t(\mathbf{n}_r \times P^j_s + P^j_r \times \mathbf{n}_s) + t^2(\mathbf{n}_r \times \mathbf{n}_s)) \cdot \mathbf{n} \\ &= \|P^j_r \times P^j_s\|(1 - t(\kappa_1 + \kappa_2) + t^2\kappa_1\kappa_2) = q(r,s)(1 - t\kappa_1(r,s))(1 - t\kappa_2(r,s)). \end{aligned} \tag{118}$$

Here we have used that the coordinate patch, P^j is C^2 hence $P^j_{rs} = P^j_{sr}$. This transformation is non-singular because of the assumption in Eq. (68)

Note that $d(\Gamma, \mathbf{x}) = t$ and denote

$$f(r,s,t) = F(X^j(r,s,t), Y^j(r,s,t), Z^j(r,s,t)). \tag{119}$$

We have

$$I_{A_j} = \int_{A_j} (\delta_\varepsilon \circ \beta^j)(F \circ \beta^j) V(D\beta^j) = \int_{r_1}^{r_2} \int_{s_1}^{s_2} \int_{-\omega}^{\omega} \delta_\varepsilon(t) f(r,s,t) q(r,s)(1 - t\kappa_1(r,s))(1 - t\kappa_2(r,s)) dt ds dr. \tag{120}$$

The assumption that $F(\mathbf{x})$ is a smooth function yields that $f(r,s,t)$ has $N+1$ bounded derivatives with respect to t. Since $t \in [-\omega, \omega]$ we can for ω small Taylor expand $f(r,s,t)$ around $(r,s,0)$

$$f(r,s,t) = \sum_{i=0}^{N} \frac{t^i}{i!} f_{it}(r,s,0) + \mathcal{O}(t^{N+1}). \tag{121}$$

The index i in f_{it} denotes the number of partial derivatives with respect to t. Define the moments of the function $\delta_\varepsilon(t)$ as

$$M_\alpha(\delta_\varepsilon(t)) = \int_{-\omega}^{\omega} \delta_\varepsilon(t) t^\alpha dt. \tag{122}$$

Replacing $f(r,s,t)$ in Eq. (120) with its Taylor expansion we obtain

$$\begin{aligned} I_{A_j} = {} & M_0(\delta_\varepsilon(t)) \int_{r_1}^{r_2} \int_{s_1}^{s_2} f(r,s,0) q(r,s) ds dr \\ & + M_1(\delta_\varepsilon(t)) \left(\int_{r_1}^{r_2} \int_{s_1}^{s_2} f_t(r,s,0) q(r,s) ds dr - \int_{r_1}^{r_2} \int_{s_1}^{s_2} f(r,s,0) q(r,s) (\kappa_1(r,s) + \kappa_2(r,s)) ds dr \right) \\ & + \sum_{\alpha=2}^{N} C^j_{\alpha,F} M_\alpha(\delta_\varepsilon(t)) + \mathcal{O}(M_{N+1}(\delta_\varepsilon(t))), \end{aligned} \tag{123}$$

where the constant $C^j_{\alpha,F}$ is given in Eq. (71).

By the change of variable $t/\varepsilon = \xi$ and since $\omega = p\varepsilon$ we get

$$M_\alpha(\delta_\varepsilon(t)) = \int_{-\omega}^{\omega} \frac{1}{\varepsilon} \varphi(t/\varepsilon) t^\alpha dt = \varepsilon^\alpha \int_{-p}^{p} \varphi(\xi) \xi^\alpha dt. \tag{124}$$

By summing up contributions from all A_j we obtain the theorem. □

References

[1] S. Osher, J.A. Sethian, Fronts propagating with curvature dependent speed: Algorithms based on Hamilton–Jacobi formulations, J. Comput. Phys. 79 (1988) 12–49.
[2] S. Osher, R. Fedkiw, Level Set Methods and Dynamic Implicit Surfaces, Springer Verlag, 2003.
[3] A.-K. Tornberg, B. Engquist, Numerical approximations of singular source terms in differential equations, J. Comput. Phys. 200 (2004) 462–488.
[4] C.S. Peskin, The immersed boundary method, Acta Numer. 11 (2002) 479–517.
[5] J. Sethian, Level Set Methods and Fast Marching Methods, Cambridge University Press, 1999.
[6] B. Engquist, A.-K. Tornberg, R. Tsai, Discretization of dirac delta functions in level set methods, J. Comput. Phys. 207 (2005) 28–51.
[7] P. Smereka, The numerical approximation of a delta function with application to level set methods, J. Comput. Phys. 211 (2006) 77–90.
[8] J.T. Beale, A proof that a discrete delta function is second-order accurate, J. Comput. Phys. 227 (2008) 2195–2197.
[9] J.D. Towers, Two methods for discretizing a delta function supported on a level set, J. Comput. Phys. 220 (2007) 915–931.
[10] J.D. Towers, A convergence rate theorem for finite difference approximations to delta functions, J. Comput. Phys. 227 (2008) 6591–6597.
[11] A.-K. Tornberg, B. Engquist, Regularization techniques for numerical approximation of pdes with singularities, J. Scient. Comp. 19 (2003) 527–552.
[12] A.-K. Tornberg, Multi-dimensional quadrature of singular and discontinuous functions, BIT 42 (2002) 644–669.
[13] E. Olsson, G. Kreiss, A conservative level set method for two phase flow, J. Comput. Phys. 210 (2005) 225–246.
[14] E. Olsson, G. Kreiss, S. Zahedi, A conservative level set method for two phase flow II, J. Comput. Phys. 225 (2007) 785–807.
[15] R.P. Beyer, R.J. Leveque, Analysis of a one-dimensional model for the immersed boundary method, SIAM J. Numer. Anal. 29 (2) (1992) 332–364.
[16] B.E. Segee, Using spectral techniques for improved performance in artificial neural networks, pp. 500–505.
[17] G. Dahlquist, Å. Björck, Numerical Methods in Scientific Computing, SIAM, 2008.
[18] P.J. Davis, P. Rabinowitz, Numerical Integration, Blaisdel Publishing Company, 1967.
[19] J.R. Munkres, Analysis on Manifolds, Westview Press, 1991.
[20] J.R. Munkres, Elementary differential topology, Princeton University Press, 1963.